STUDY OF WEAR MECHANISMS OF DELTA ROOF REFRACTORIES IN EAF

Simon Chiartano, Dr Pascal Prigent, Dr Sébastien Pinard
TRB, Engineering Department, Decines France

Abstract

The wear mechanisms of refractories used in a delta roof were investigated in this paper. TRB Company used its skills and expertise to understand the wearing process of this sensitive component, including some innovative tools: immersive measurement by thermocouples, IR thermal camera, 3D laser scanner, thermomechanical numerical simulation, SEM, X-ray fluorescence, X-ray diffraction. This presentation is following one particular delta installed at one of our customers on which the whole study has been carried out.

Introduction

One of the most common technologies used in steel-making industries is the Electric Arc Furnace (EAF). The EAF consists of a refractory-lined vessel, covered with a roof. The centre of the roof is called the delta and made of a refractory product. For the past 20 years, TRB has designed and produced deltas for the EAF. The delta is composed of a refractory precast shape.

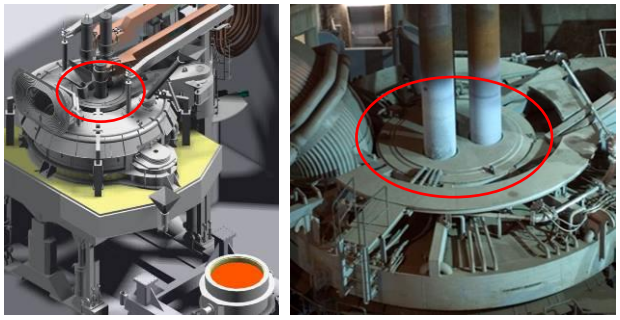

Fig. 1: EAF design [1]- delta roof red circled.

The wear mechanisms of delta roofs are not well known. This is one of the most affected parts of the EAF as it is subject to all kinds of stresses, e.g. thermal, chemical and mechanical (see Figure 2). The delta bottom surface is exposed to temperature by radiation and slag splashes. It is also exposed to the corrosive action of slag and metal oxides. Due to the complicated design of the delta that has to encompass openings for the electrodes, water cooling arrangements, etc. it is subjected to considerable mechanical stresses and thermal shocks causing deterioration of the refractory.

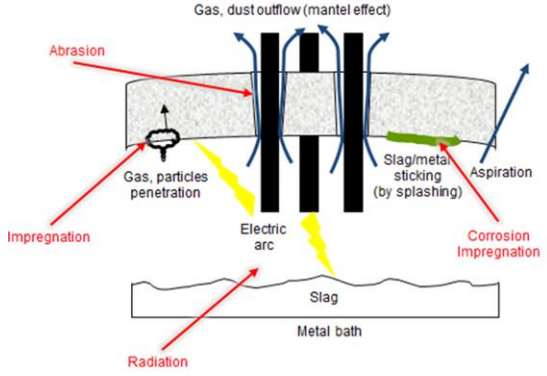

Fig.2: EAF delta roof stress.

Material and methods

Thermal measurement

In order to contribute to a better knowledge of the processes of degradation, temperature measurements of a delta roof were performed over several campaigns of the deltas. Measurements were made in different heights and positions using 11 K-type thermocouples and a data logger to record temperatures (see Figure 3 & 4).

Fig. 3: Thermocouples introduction in delta roof.

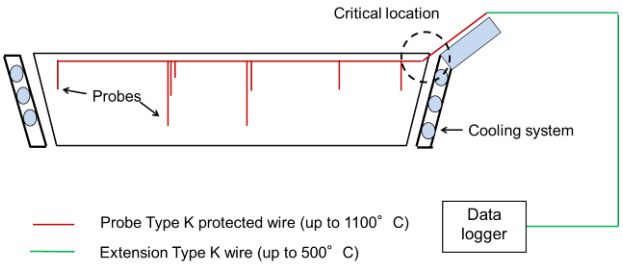

Fig. 4: Thermocouples location in delta roof.

To complete the measurement, a thermal camera was used to get the delta bottom temperature. The measure was taken just after the opening of the EAF.

Numerical simulation

A numerical simulation using finite element analysis helps us to understand the thermomechanical behaviour of the delta in operation. This study consists of a transient fully-coupled calculation: thermal and mechanical. The thermal boundaries consider the radiation and/or convection of the melting slag, electrodes, ambient air and cooling system on the delta. The mechanical boundaries only consider the ferrule around the delta. See Table 1.

Tab. 1: Numerical simulation boundaries.

Thermal boundary	Mechanical boundary	Location
Cyclic radiative exchange with electrodes and melting slag	Free	
Convective and radiative exchange with ambient air	Free	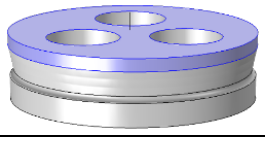
Convective exchange with water	Planar linkage	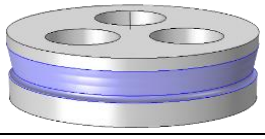

The meshing of the delta design consists of 31112 tetrahedral elements, see Figure 6.

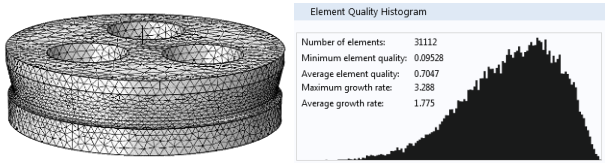

Fig. 6: Numerical simulation meshing.

Wear measurement

TRB uses a 3D laser scanner to have an exact idea of the wear of the delta roof. The scanner allows precise as well as fast measuring on any type of part or structure. The superposition of several point clouds edited on different dates gives an accurate estimate of the wear thickness and also the remaining refractory lining.

Post mortem analysis

The samples were collected on the hot face of the instrumented delta roof after use. Figure 7 shows a view of corroded samples and different analysed zones: in contact with an electrode (a), in contact with the slag (b).

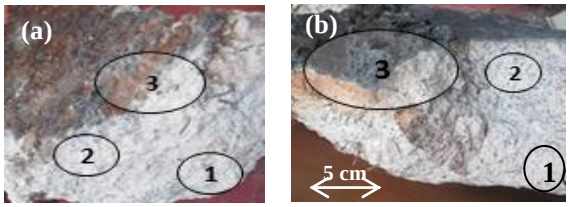

Fig. 7: Corroded samples collected for post mortem analyses.

Zone 3 corresponds to the interface slag/refractory. In the both samples, zone 1 and 2 respectively located at ten and one centimetre from the hot face match those no-corroded castable (confirmed by X-ray measurements in table 2).

Results and Discussion

Thermal measurement

The data logger recorded the 11 thermocouples temperature during the 180 first hours of the delta roof's life. See Figures 8 & 9.

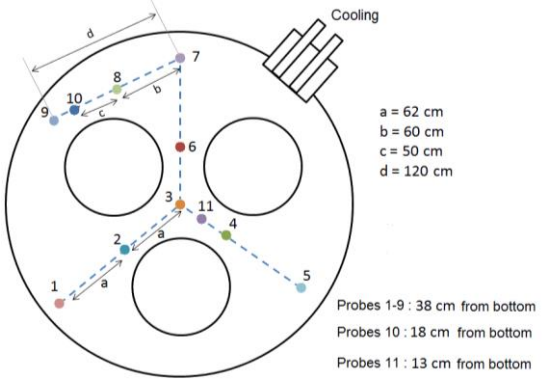

Fig. 8: Probes location.

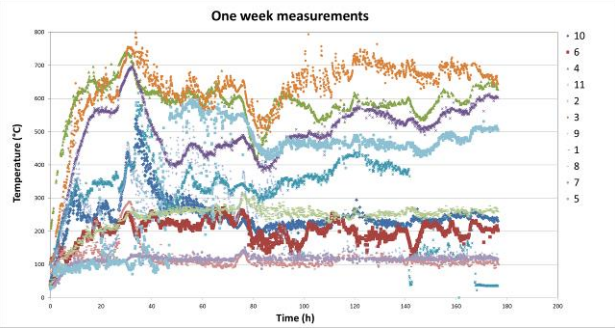

Fig. 9: Probes results during one week.

Using a thermal camera, a thermography (Figure 9) was made under the delta just after its removal of the roof. We can still see the electrode end inside the holes. This measure was taken on a delta relatively new.

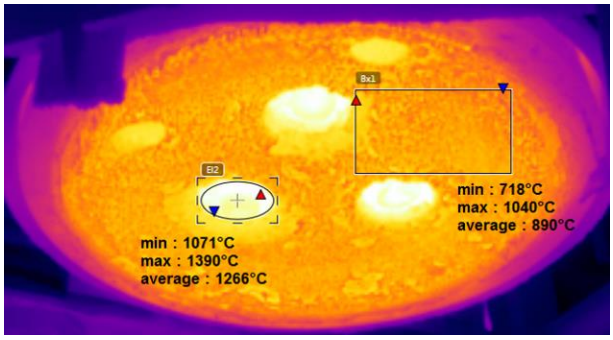

Fig. 10: Thermography of the delta roof's bottom.

Numerical simulation

The simulation study the delta roof's behaviour during the first 40 hour's lifetimes. Figure 11 shows temperature profile in 3 cut planes: centred vertical (Fig. 11-1), across two holes vertical (Fig. 11-2) and middle height horizontal i.e. 38 centimetres from the bottom (Fig. 11-3). Temperature results indicate rather low temperature distribution. For the majority of the delta, temperature is under 600°C. This can be explained by the cooling of the ferrule.

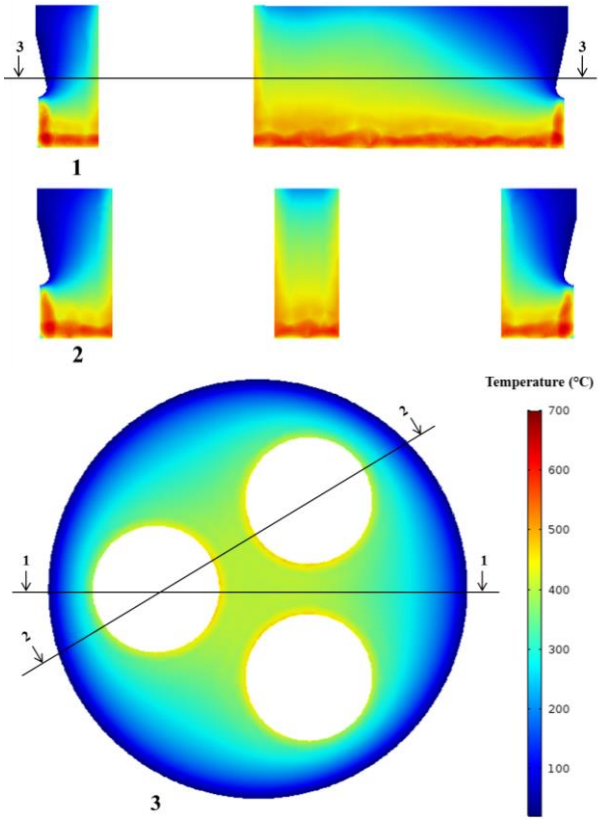

Fig. 11: Simulation results after 40 hours: temperature (°C).

On the bottom face, the temperature is of course depending on the heating cycles, but it varies from 500 to 1050°C. This temperature level under the delta is quite low regarding previous studies:

- Chan : 1027 °C [6]
- Henning : 1527 °C [9]
- Pfeifer : 1027 °C to 1327 °C [4]
- Gruber : 1027 °C [7]
- Guo : 1032 to 1400 °C [5]

In these references the delta's temperature wasn't the final aim of the simulation and sometimes the roof temperature was just assumed ([6], [9]). In other cases, the cooling of the roof wasn't take into account [5] this explains easily higher thermal results.

Thermomechanical Von Mises stress results (Fig. 12) show a distribution consistent with thermal profile. One could see that the ferrule limitation doesn't have much effect on the stresses. As the delta is free to move above and below this restriction doesn't make any stress concentration. On the other hand, maximum stresses are reached around and between electrode holes. Here, stress level is even higher than on the bottom face.

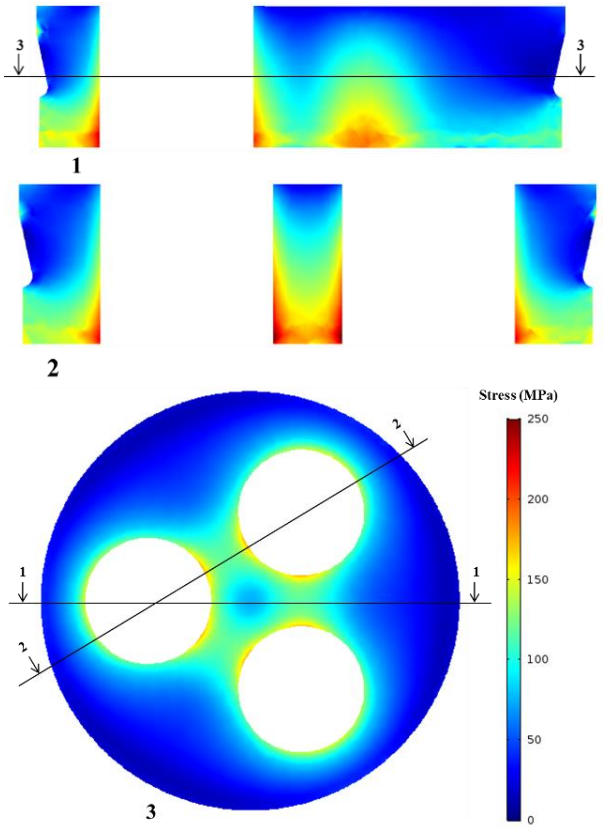

Fig. 12: Simulation results after 40 hours: VM stresses (MPa).

A correlation was performed to get a validation of the simulation. Figure 13 show transient results on points 1, 2, 8 and 11 with solid outlines for thermocouples measurement and dashed outlines for simulation. Results are reasonable and consistent. Measured values are more variable, but generally speaking, temperature level is the same in average. The difference can be explained by the process conditions which are more fluctuating rather than periodic cycles consider in the simulation.

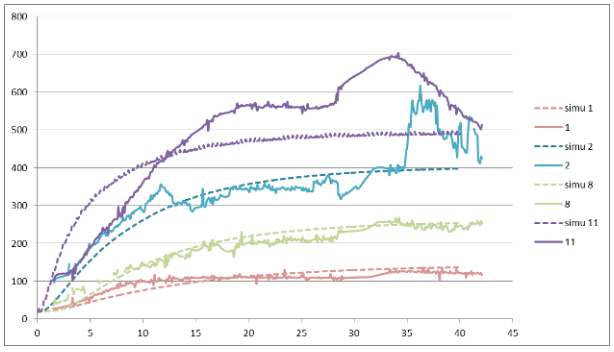

Fig. 13: Thermal correlation between thermocouples measurement (solid outlines) and simulation (dashed outlines).

Wear measurement

A 3D scan was carried out to get an accurate measure of the delta wear. Figure 14 shows the point cloud of a new delta roof. This technique confirms the thermos-mechanical results: most of the times, maximum wear is located near the electrode holes.

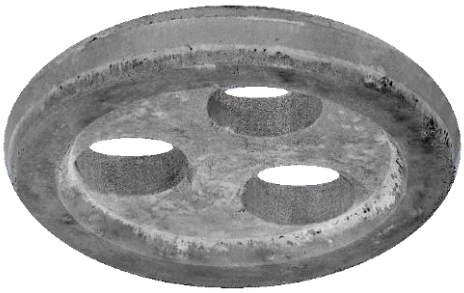

Fig. 14: Point cloud of the roof delta (new).

The classic wear profile of the delta roof at the end of a campaign is shown on Figure 15. The general wear shape of the bottom (dashed red line) is in good correlation with the simulation thermos-mechanical profile (Figure 12-1).

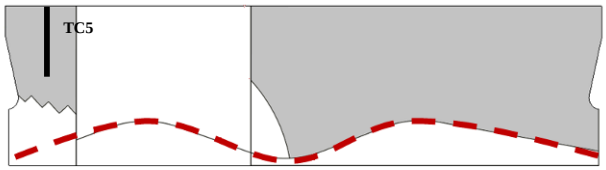

Fig. 15: Typical wear profile of the delta at a campaign's end.

Around the electrode holes, wear is important as sometimes, the precast shape can fracture and break off. Near thermocouple number 5, after approximatively 45 hours, a collapsing of a piece of castable occurs close to a delta hole. See Figure 16.

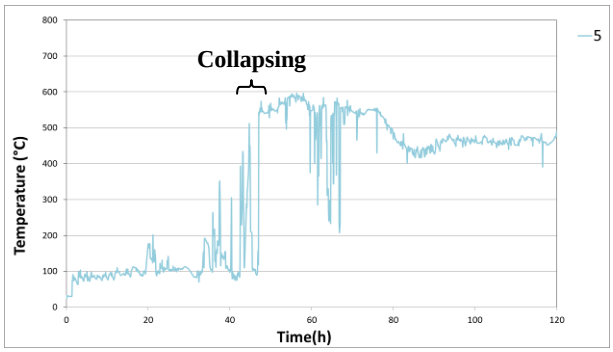

Fig. 16: Collapsing of a piece castable near TC 5.

Post mortem analysis

Table 2 shows the chemical analysis in different zones 1, 2 & 3. The chemical analysis, performed on the hot face (zone 3), highlights an important content of iron oxide. As the chemical composition of the slag has a high lime content (table 2) it proves that the hot face isn't in contact with slag. The thin layer that can be seen on the samples is mostly steel deposition. The value of open porosity and bulk density are closed to the reference castable this confirms that the material is not corroded by slag.

Tab. 2: Chemical analyses by XRF.

		Reference castable	Corroded sample						Slag
			a			b			
Bulk density		2640 at 110°C	2760			2677			
Open porosity		13 at 110°C	13,7			15,4			
Zone			1	2	3	1	2	3	
Assays (%)	Al_2O_3	63	63,2	63	2,5	62,2	63,3	1,9	
	SiO_2	30	29,5	29,4	8	29,5	29,4	7,6	33,8
	TiO_2	1,4	1,8	1,9	0,2	1,8	1,9	0,5	2,2
	Fe_2O_3	0,9	1,2	1,3	65	0,9	1,2	61,5	2,7
	CaO	0,5	0,5	0,5	6,1	0,4	0,7	8,4	44
	ZrO_2	4,1	3	3,3		4,2	3,3		
	K_2O	<0,3	0,2	0,2		0,2	0,2		
	MnO								1,1
	MgO								12
	Cr_2O_3								4,2

Table 3 shows the major and minor mineralogical phases detected by X-ray measurements. In both samples, phases correspond to a no-corroded refractory as the castable used in this study is mainly composed of mullite.
In both samples, andalousite content in zone 1 & 2 remains substantial. The presence of andalusite in samples proves that the temperature is less than 1300°C as the beginning of mullitization of the andalousite started at this temperature [2]. Moreover, anorthite has also been found in all zones. The crystallization of anorthite occurs between 900°C and 1100°C [10] so the temperature reached at least 900°C in the samples.

Tab. 3: Mineralogical analyses by X-ray diffraction.

Main phases	a		b	
	Zone 1	Zone 2	Zone 1	Zone 2
Corundum	+++	+++	+++	+++
Mullite	++++	++++	++++	++++
Baddeleyite	+	+	+	+
Andalusite	++	++	++	++
Quartz	+	+	+	+
Zircon	--	--	--	--
Anorthite	+	+	+	+

Therefore, the temperature range on the hot face of the delta roof is between 900°C and 1300°C.

Conclusions

The TRB Company uses all the controls it has available to improve its comprehension of wear mechanisms in the EAF delta roof.
Thermal measurements were performed inside the refractory and on its skin. Results show relatively low temperature level, with less than 600°C inside the delta and a maximum of 1050°C on the hot face.
A numerical simulation confirms these data and explains the thermal profile by the cooling of the ferrule. This calculation also informs us about locations where thermomechanical stresses are critical.
Wear measurements using 3D scan corroborate the simulation by pointing out the electrode holes to be the delta roof critical area.
Finally, a post mortem analysis made on 3 different zones on 2 samples was undertaken. XRF and XRD results prove that the slag corrosion isn't significant. Those tests also show that the bottom temperature of the delta should be between 900 and 1300°C, which is in accordance with the thermal calculation.

As a consequence, a new refractory recipe was developed in order to increase mechanical properties at low temperature (<1200°C). Compared to reference castable, the mechanical resistance (after firing at 1000°C) was increased by 40 MPa. Furthermore, the open porosity was reduced by 4% and the thermal shock resistance performed at 1000°C was twice higher than the reference. We look forward to installing this new promising product to our customer.

References

[1] **Siemens global Website**: Simetal EAF FAST DRI Siemens. http://www.siemens.com/press/pool/de/feature/2012/industry/metals-technologies/2012-03-steel/simetal-eaf-fast-dri-en.pdf
[2] **Bouchetou M.L.; Poirier J.; Ildefonse J.P.; Hubert P.**: Kinetics of Mullitization of Andalusite Crystals and Role of the Transformations at High Temperature of the Minor Mineral Inclusions, pp. 360-366
[3] **Wang, T.; Liu, B.**: The factors effecting on the service life of HP/UHP EAF roof ; UNITECR 2003, pp. 557-559.
[4] **Pfeifer, H.; Echterhof, T.; Voj, L.; Gruber, J.; Jung, H.-P.; Lenz, S.; Beiler, C.; Cirilli, F.; De Miranda, U.; Veneri, N.; Bressan, E.**: EUR 25078 - Control of nitrogen oxide emission at the electric arc furnace - CONOX, European Commission, Luxembourg, (2012), pp. 92 - 126
[5] **Guo, D.; Irons, G.**: Radiation Modeling in an EAF, AISTech 2004 Proceedings, Vol. 1, pp. 991-999
[6] **Chan, E.; Riley, M.; Thomson, M.J.; Evenson, E.J.**: Nitrogen Oxides (NOx) Formation and Control in an Electric Arc Furnace (EAF): Analysis with Measurements and Computational Fluid Dynamics (CFD) Modeling, ISIJ Int., 44 (2004), pp. 429 - 438
[7] **Gruber, J. C.**: Development of a Numerical Model for the Heat and Mass Transport in an Electric Arc Furnace Freeboard, Faculty of Georesources and Materials Engineering of the RWTH Aachen University
[8] **Arzpeyma, N.**: Modeling of Electric Arc Furnaces (EAF) with electromagnetic stirring, School of Industrial Engineering and Management Department of Materials Science and Engineering, Stockholm
[9] **Henning, B.; Shapiro, M.; le Grange, L.A.**: DC Furnace Containment Vessel Design using Computational Fluid Dynamics, Proc. of 10th International Ferroalloys Congress, SAIMM, Johannesburg, (2004), pp. 565 – 574
[10] **Klein L.; Uhlmann D. R.:** Crystallization behavior of anorthite, JCR, November 1974